

Supporting Information

pH-controlled assembly of $[ZnW_{12}O_{40}]^{6-}$ -based hybrids from 0D dimer to 2D network: synthesis, crystal structure, and photocatalytic performance in transformation of toluene into benzaldehyde

Ke-Ke Guo, Yan-Li Yang, Xin-Ye Jiang, Feng-Yan Li*, Si-Meng Dong, and Lin Xu*

Key Laboratory of Polyoxometalate and Reticular Material Chemistry of Ministry of Education, Faculty of Chemistry, Northeast Normal University, Changchun, Jilin 130024, P. R. China.

E-mail: linxu@nenu.edu.cn; lify525@nenu.edu.cn

Table S1. Selected bond lengths (Å) and bond angles (°) of **1-3**.

Compound 1			
Zn1-O34	1.866(13)	Cu1 ⁱ -O5	2.270(14)
Zn1-O37	1.841(13)	Cu2-O2	1.936(13)
Zn1-O35	1.856(14)	Cu2-O42	2.015(13)
Zn1-O36	1.893(13)	Cu2-O41	2.246(13)
Cu1-N1	2.022(17)	Cu2-N3	1.969(17)
Cu1-N2	1.974(18)	Cu3-O43	1.943(18)
Cu1-O51	1.968(14)	Cu3-O44	1.974(17)
Cu1-O5 ⁱ	2.270(14)	Cu3-O45	2.268(17)
Cu1-O1	1.976(13)	Cu3-N5	1.974(18)
O35-Zn1-O36	108.6(6)	O2-Cu2-N5	92.8(7)
O35-Zn1-O34	107.9(6)	O2-Cu2-N6	152.4(16)
O37-Zn1-O36	108.3(6)	O2-Cu2-N7	105.2(18)
O37-Zn1-O35	111.1(6)	O2-Cu2-N8	94.2(10)
O37-Zn1-O34	109.5(6)	O1-Cu1-O5 ⁱ	109.4(5)
O34-Zn1-O36	111.4(6)	O1-Cu1-N1	154.3(6)
O2-Cu2-O42	88.0(5)	O51-Cu1-O1	86.4(6)
O2-Cu2-O41	101.2(5)	O51-Cu1-O5 ⁱ	88.0(6)
O2-Cu2-N3	93.9(7)	O51-Cu1-N2	176.5(7)
O2-Cu2-N4	169.5(6)	O51-Cu1-N1	97.8(6)
O42-Cu2-O41	89.7(5)	N2-Cu1-O1	95.7(6)
N3-Cu2-O42	169.8(6)	N2-Cu1-O5 ⁱ	88.6(6)
N3-Cu2-O41	99.7(6)	N2-Cu1-N1	81.6(7)
N3-Cu2-N4	83.0(7)	N1-Cu1-O5 ⁱ	96.1(6)
N4-Cu2-O42	93.3(6)	N6-Cu3-N5	81.4(7)
N4-Cu2-O41	89.2(6)	N6-Cu3-O44	95.3(8)
Symmetry codes: (i) -x+1, -y, -z+1.			
Compound 2			
Zn1-O40	1.901(17)	Cu1-O41	1.95(2)
Zn1-O38	1.903(16)	Cu2-O43	1.98(2)
Zn1-O39	1.891(15)	Cu2-O44	1.97(2)
Zn1-O37	1.906(17)	Cu2-N3	2.02(3)
Cu1-O22	1.967(18)	Cu2-O42	2.33(3)
Cu1-N1	2.04(2)	Cu2-N4	1.98(3)
Cu1-N2	2.00(3)	O17-Cu1 ⁱⁱ	2.24(2)
Cu1-O17 ⁱ	2.24(2)		
O40-Zn1-O38	111.0(7)	O39-Zn1-O40	107.7(7)
O40-Zn1-O37	109.2(7)	O39-Zn1-O38	109.7(7)
O38-Zn1-O37	110.2(7)	O39-Zn1-O37	109.1(7)
O22-Cu1-N1	169.3(8)	O43-Cu2-N3	168.6(10)
O22-Cu1-N2	94.0(9)	O43-Cu2-O42	94.7(11)

O22-Cu1-O17 ⁱ	102.1(7)	O44-Cu2-O43	91.4(10)
N1-Cu1-O17 ⁱ	87.7(8)	O44-Cu2-N3	94.4(10)
N2-Cu1-N1	80.1(11)	O44-Cu2-O42	89.4(11)
N2-Cu1-O17 ⁱ	98.8(9)	O44-Cu2-N4	175.6(10)
O41-Cu1-O22	88.2(8)	N3-Cu2-O42	95.2(11)
O41-Cu1-N1	95.4(10)	N4-Cu2-O43	92.7(10)
O41-Cu1-N2	165.9(11)	N4-Cu2-N3	81.8(10)
O41-Cu1-O17 ⁱ	94.4(10)	N4-Cu2-O42	88.7(11)
Symmetry codes: (i) $-x+1/2, y-1/2, z$; (ii) $-x+1/2, y+1/2, z$.			
Compound 3			
Zn1-O35	1.890(8)	Cu2-O43	2.018(8)
Zn1-O33	1.884(8)	Cu2-O5 ⁱ	2.323(8)
Zn1-O36	1.845(8)	Cu2-N3	1.981(9)
Zn1-O34	1.821(8)	Cu2-N4	1.985(9)
Cu1-O39 ⁱⁱ	1.930(8)	O5-Cu2 ⁱⁱⁱ	2.323(8)
Cu1-O1	1.946(8)	Cu3-O42	1.954(9)
Cu1-N1	2.003(10)	Cu3-N5	1.968(11)
Cu1-N2	1.985(9)	Cu3-N6	1.998(10)
O39-Cu1 ⁱⁱ	1.930(8)	Cu3-O41	1.971(11)
Cu2-O2	1.967(8)		
O33-Zn1-O35	112.6(4)	O2-Cu2-O43	86.4(3)
O36-Zn1-O35	109.5(4)	O2-Cu2-O5 ⁱ	103.3(3)
O36-Zn1-O33	106.0(4)	O2-Cu2-N3	94.0(4)
O34-Zn1-O35	107.5(4)	O2-Cu2-N4	171.7(4)
O34-Zn1-O33	110.6(4)	O43-Cu2-O5 ⁱ	84.6(3)
O34-Zn1-O36	110.7(4)	N3-Cu2-O43	167.5(4)
O39 ⁱⁱ -Cu1-O1	90.6(3)	N3-Cu2-O5 ⁱ	107.4(3)
O39 ⁱⁱ -Cu1-N1	175.6(4)	N3-Cu2-N4	82.3(4)
O39 ⁱⁱ -Cu1-N2	94.9(4)	N4-Cu2-O43	95.6(4)
O1-Cu1-N1	93.6(4)	N4-Cu2-O5 ⁱ	84.9(3)
O1-Cu1-N2	174.5(4)	O42-Cu3-N5	169.0(4)
N2-Cu1-N1	81.0(4)	N5-Cu3-N6	82.2(4)
O42-Cu3-N6	92.5(4)	N5-Cu3-O41	91.4(5)
O42-Cu3-O41	91.4(4)	O41-Cu3-N6	164.9(4)
Symmetry codes: (i) $-x+1/2, y-1/2, -z+1/2$; (ii) $-x+1, -y+1, -z+1$.			

Table S2. Continuous shape measures calculation for the Cu²⁺ ions in **1-3**.

Metal ions	Label	Symmetry	Shape	CShM value
Cu1 in 1	PP-5	D_{5h}	Pentagon	29.895
	vOC-5	C_{4v}	Vacant octahedron	2.438
	TBPY-5	D_{3h}	Trigonal bipyramid	2.509
	SPY-5	C_{4v}	Spherical square pyramid	2.030
	JTBPY-5	D_{3h}	Johnson trigonal bipyramidal J12	5.863
Cu1 in 2	PP-5	D_{5h}	Pentagon	30.516
	vOC-5	C_{4v}	Vacant octahedron	2.269
	TBPY-5	D_{3h}	Trigonal bipyramid	2.516
	SPY-5	C_{4v}	Spherical square pyramid	2.021
	JTBPY-5	D_{3h}	Johnson trigonal bipyramidal J12	6.912
Cu2 in 3	PP-5	D_{5h}	Pentagon	24.551
	vOC-5	C_{4v}	Vacant octahedron	1.954
	TBPY-5	D_{3h}	Trigonal bipyramid	6.251
	SPY-5	C_{4v}	Spherical square pyramid	1.572
	JTBPY-5	D_{3h}	Johnson trigonal bipyramidal J12	9.078

Table S3. The bond-valence sum (BVS) calculations of W, Zn and Cu for **1-3**.

Compound 1		Compound 2		Compound 3	
Atom	Oxidation states	Atom	Oxidation states	Atom	Oxidation states
W1	6.20	W1	5.75	W1	6.17
W2	6.16	W2	6.05	W2	6.06
W3	6.12	W3	5.94	W3	6.14
W4	5.95	W4	6.04	W4	6.08
W5	6.07	W5	5.80	W5	6.18
W6	5.99	W6	5.95	W6	6.20
W7	6.16	W7	6.09	W7	6.02
W8	6.15	W8	6.25	W8	5.99
W9	6.08	W9	6.22	W9	5.97
W10	6.11	W10	6.15	W10	6.00
W11	6.10	W11	6.15	W11	6.15
W12	6.13	W12	6.14	W12	6.07
Zn1	2.66	Zn1	2.35	Zn1	2.69
Cu1	2.08	Cu1	2.04	Cu1	1.91
Cu2	2.12	Cu2	2.01	Cu2	2.02
Cu3	2.16			Cu3	1.91

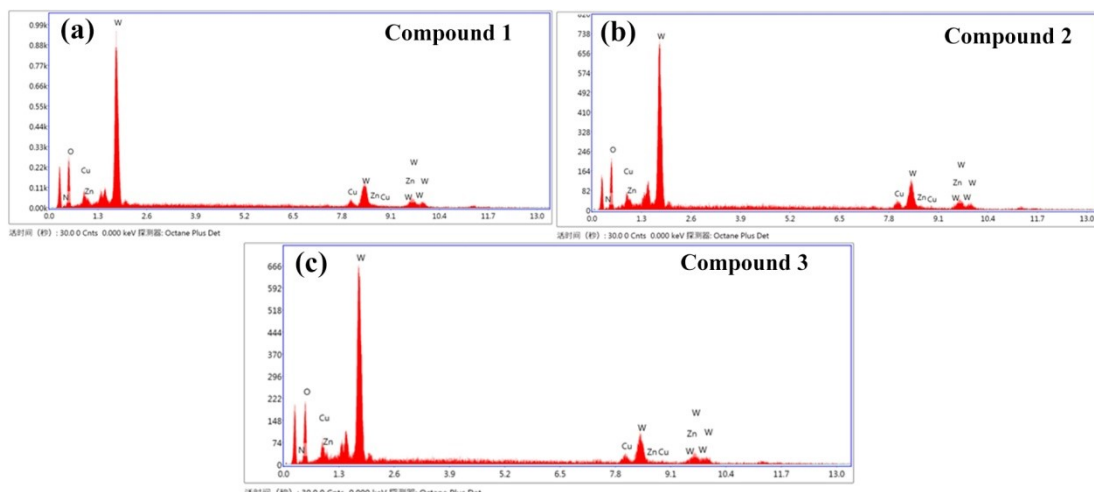
Table S4. Summary of the photocatalytic toluene oxidation over many photocatalysts.

Catalyst	Substrate	T/°C	Light source	Solvent	Oxidant	Conv. /%	Sel. /%	Ref.
<i>p</i> -BWO	1 mmol	RT	> 400 nm	CH ₃ CN	O ₂	97	91	1
WO ₃ /TiO ₂	50 μmol	RT	> 300 nm	CH ₃ CN	O ₂	50	50	2
CdS	0.2 mmol	60	visible light	CH ₃ CN	O ₂	13	52.5	3
Bi ₂ WO ₆	8 mmol	RT	visible light	none	O ₂	0.5	95	4
Nb ₂ O ₅ -N	0.1 mmol	40	455 nm	CH ₃ CN	O ₂	1.56	96	5
NbBA	1 mmol	30	UV	none	O ₂	27	54	6
		45	visible light	none	O ₂	15	70	
Fe-UiO-66	50 μmol	RT	UV	CH ₃ CN	O ₂	70.1	19.3	7
Compound 3	1 mmol	RT	> 420 nm	CH ₃ CN	O ₂	17.3	97.6	This work

RT: room temperature; BA: benzyl alcohol.

Table S5. Photocatalytic oxidation of toluene under different catalysts.

Entry	Catalyst	t/h	Atm	Conv. (%)	Sel. (%)
1	(Me ₄ N) ₆ [ZnW ₁₂ O ₄₀]·9H ₂ O	12	O ₂	2.3	25.0
2	[Cu(bipy)(H ₂ O) ₃]·(NO ₃) ₂	12	O ₂	< 1	-

**Fig. S1** Energy dispersive X-ray spectroscopy (EDS) of 1 (a), 2 (b) and 3 (c), respectively.

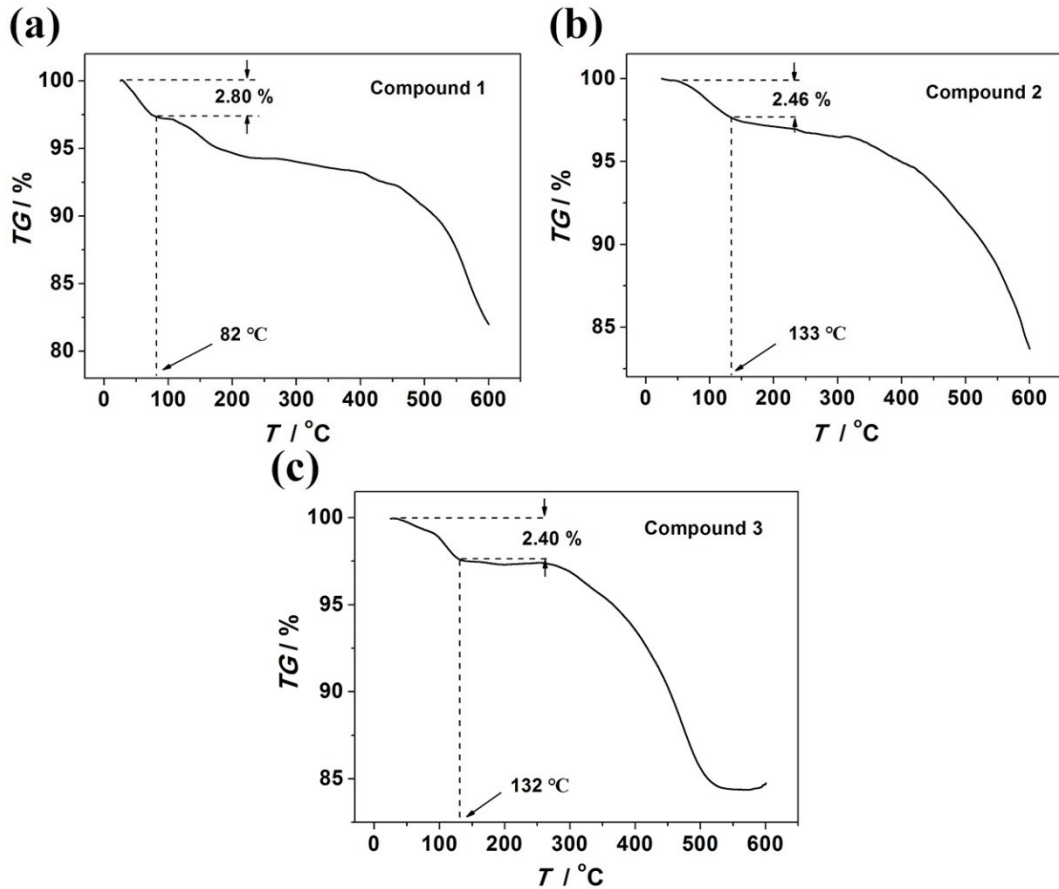


Fig. S2 TGA curves of **1** (a), **2** (b) and **3** (c), respectively.

The thermogravimetric analysis (TGA) of compound **1** (Fig. S2a) shows that it went through a weight loss of 2.80 % in the temperature range of 25–82 °C, corresponding to the weight loss of six free lattice H₂O molecules (calc. 2.87%); this result is consistent with the content of H in free lattice water by elemental analysis. After that, its framework started to collapse with a series of complicated weight losses. For compound **2-3**, the thermogravimetric (TG) behaviors are very similar to each other. Herein only the TG behavior of **3** is described as the representatives. TGA of **3** (Fig. S2c) shows that it went through a weight loss of 2.40 % in the temperature range of 25–132 °C, corresponding to the weight loss of five free lattice H₂O molecules (calc. 2.44%); this result is also consistent with the content of H in free lattice water by elemental analysis. Then, its framework kept stable until approximately 270 °C. After that, its framework started to collapse with a series of complicated weight losses.

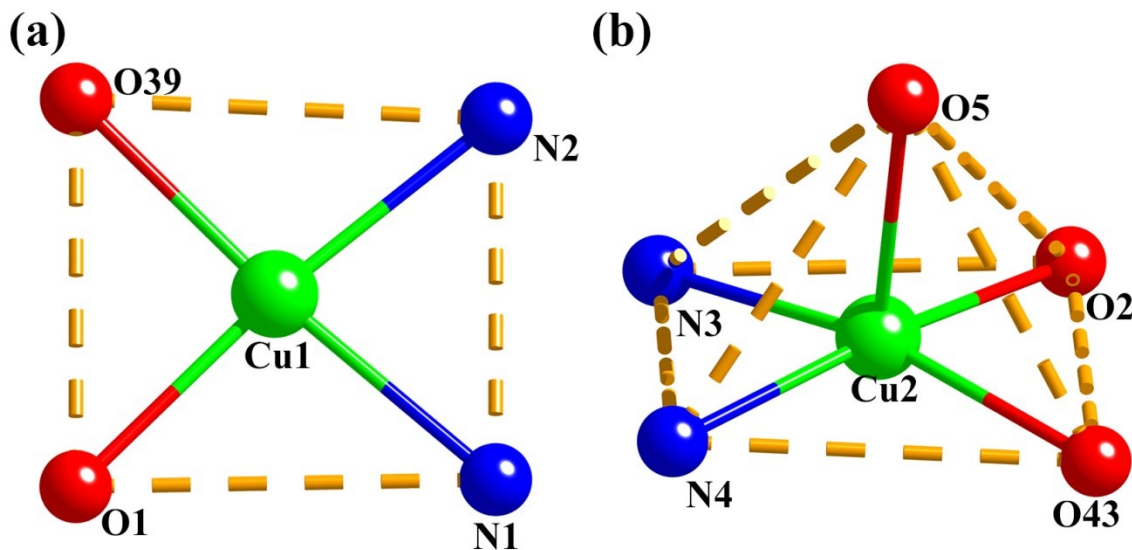


Fig. S3 Coordination geometries of Cu1 and Cu2, respectively, of compound **3**.

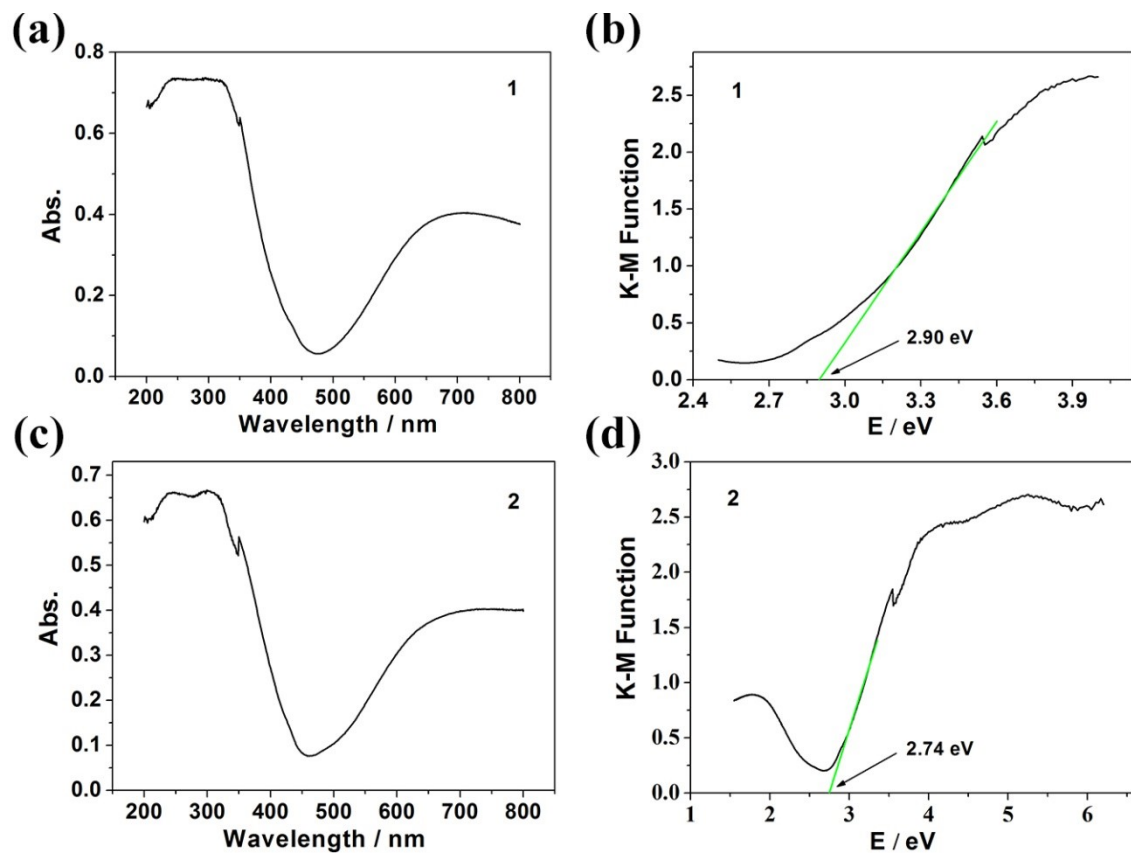


Fig. S4 UV-vis diffuse reflectance spectra of **1** (a) and **2** (c) respectively, diffuse reflectance UV-vis-NIR spectra of K-M functions versus energy (eV) of **1** (b) and **2** (d).

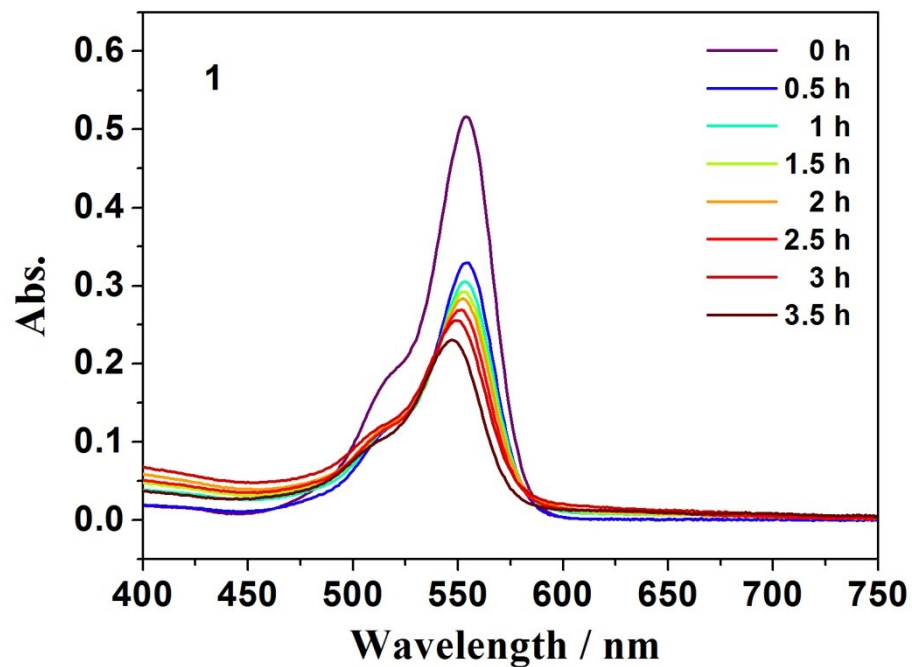


Fig. S5 Absorption spectra of RhB solution in the presence of **1** under visible light.

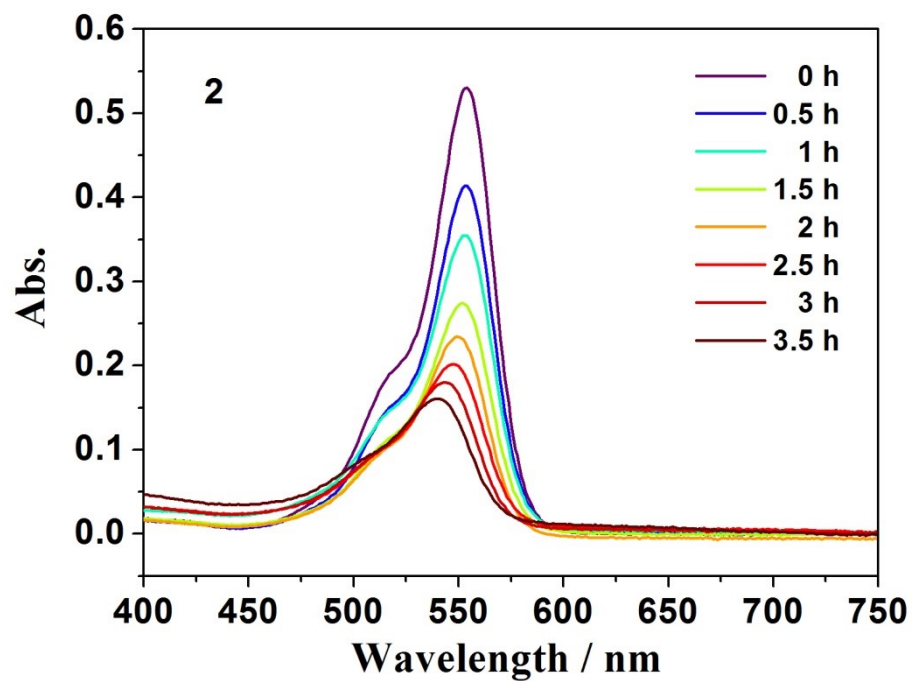


Fig. S6 Absorption spectra of RhB solution in the presence of **2** under visible light.

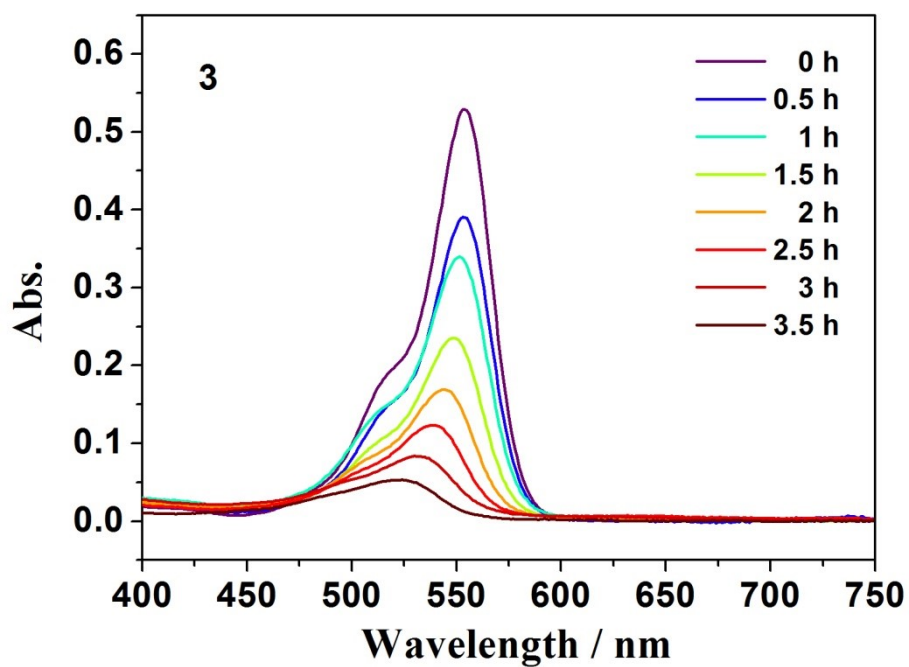


Fig. S7 Absorption spectra of RhB solution in the presence of **3** under visible light.

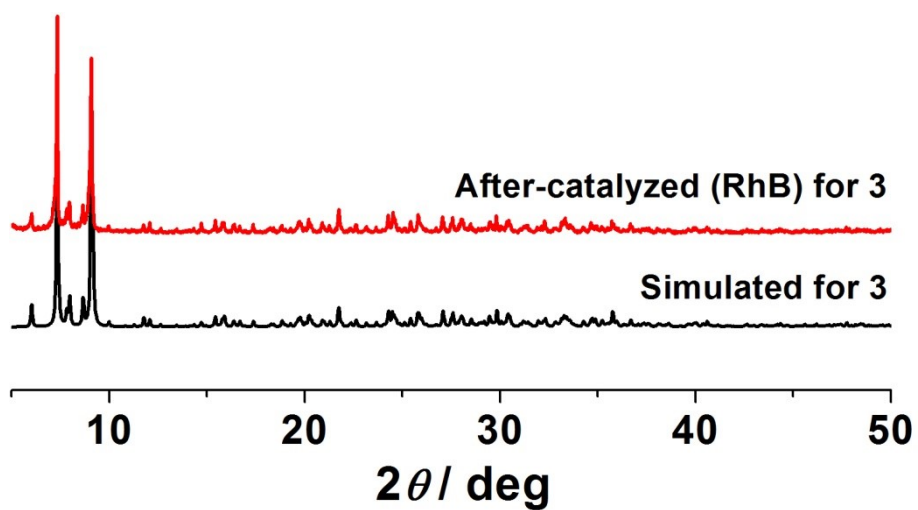


Fig. S8 PXRD patterns of **3** after (red) photocatalytic degradation of RhB and its simulated one (black).

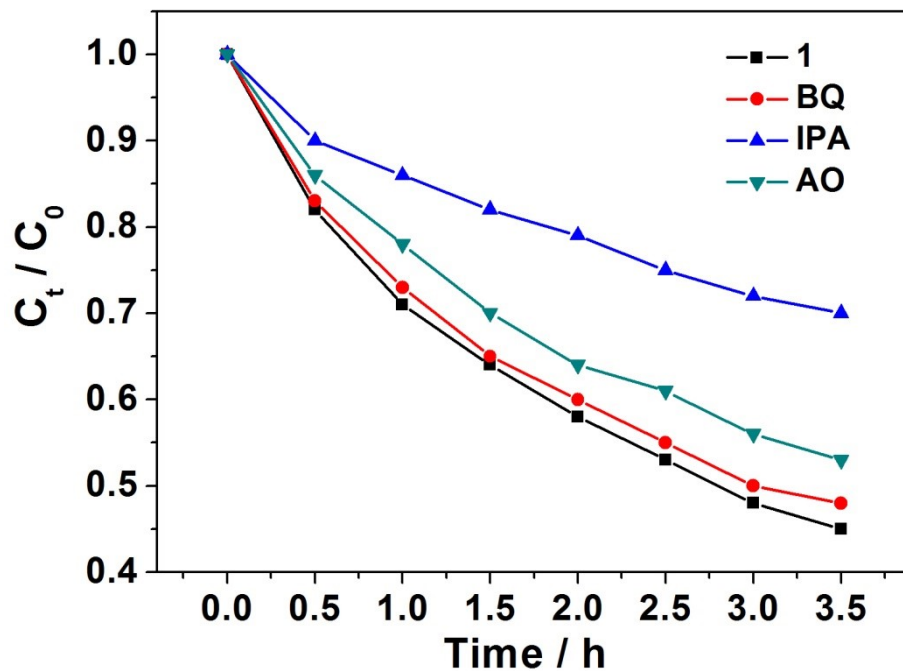


Fig. S9 Photocatalytic degradation of RhB by **1** in the presence of different radical scavengers.

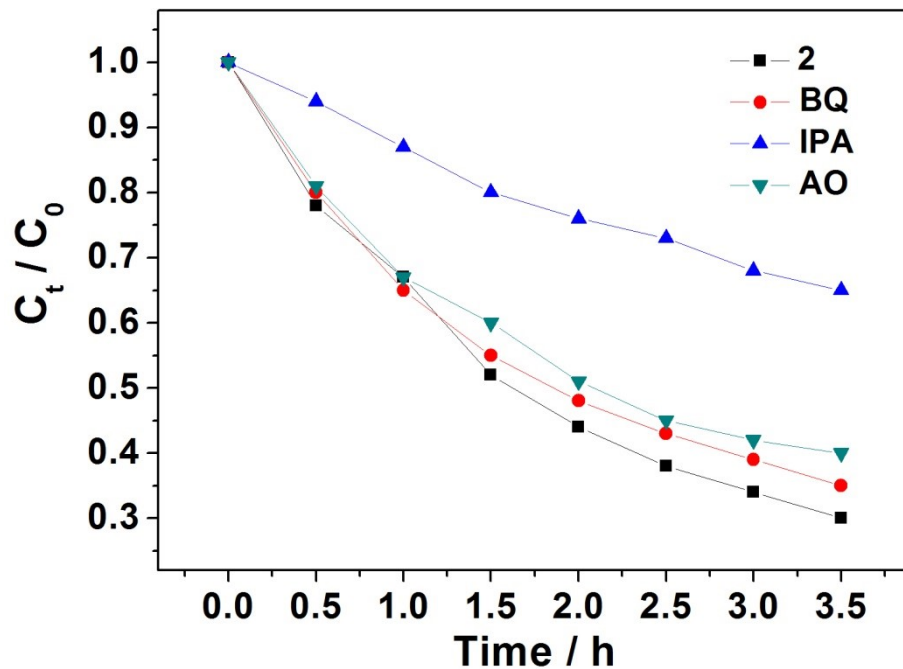


Fig. S10 Photocatalytic degradation of RhB by **2** in the presence of different radical scavengers.

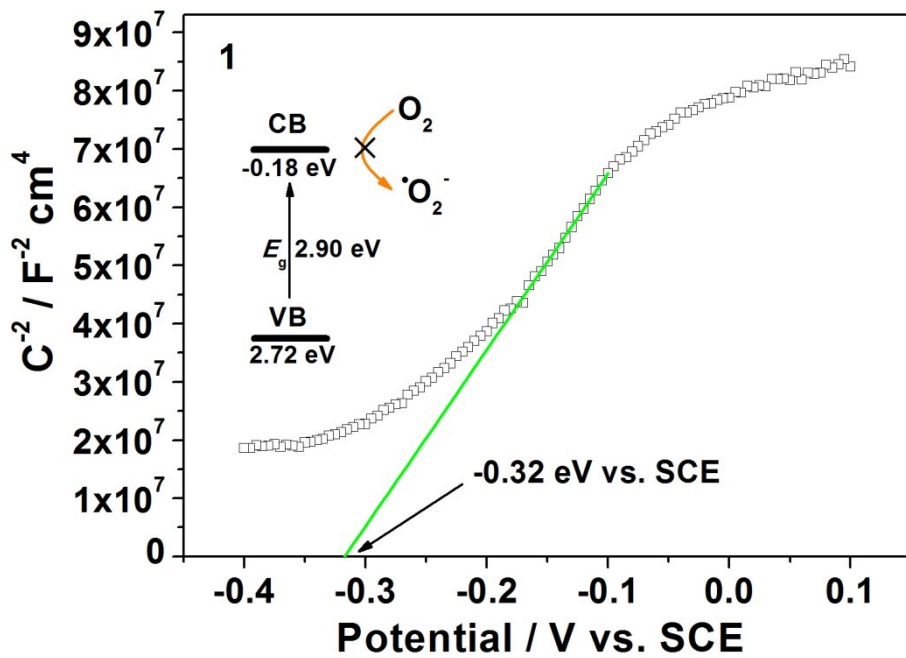


Fig. S11 Mott-Schottky plot of **1** at a frequency of 1.0 kHz.

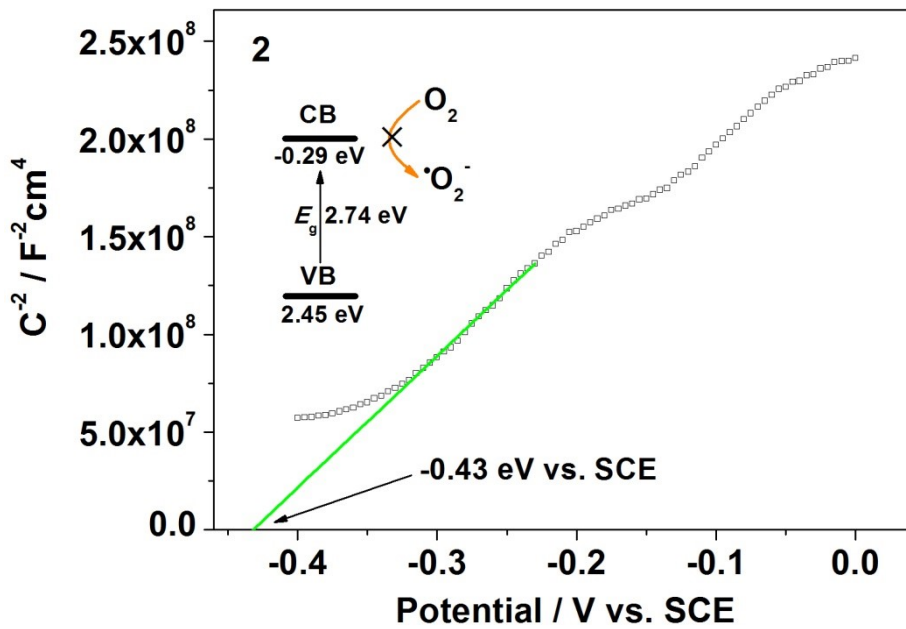


Fig. S12 Mott-Schottky plot of **2** at a frequency of 1.0 kHz.

References

- 1 X. Cao, Z. Chen, R. Lin, W.C. Cheong, S. Liu, J. Zhang, Q. Peng, C. Chen, T. Han, X. Tong, Y. Wang, R. Shen, W. Zhu, D. Wang and Y. Li, *Nat. Catal.*, 2018, **1**, 704-710.
- 2 D. Tsukamoto, Y. Shiraishi and T. Hirai, *Catal. Sci. Technol.*, 2013, **3**, 2270-2277.
- 3 G. Zhao, B. Hu, G. Wilma-Busser, B. Peng and M. Muhler, *ChemSusChem.*, 2019, **12**, 2795-2801.

- 4 Y. Liu, L. Chen, Q. Yuan, J. He, C.T. Au and S.F. Yin, *Chem. Commun.*, 2016, **52**, 1274-1277.
- 5 K. Su, H. Liu, B. Zeng, Z. Zhang, N. Luo, Z. Huang, Z. Gao and F. Wang, *ACS Catal.*, 2020, **10**, 1324-1333.
- 6 S. Sarina, H. Zhu, Z. Zheng, S. Bottle, J. Chang, X. Ke, J. C. Zhao, Y. Huang, A. Sutrisno, M. Willansc and G. Li, *Chem. Sci.*, 2012, **3**, 2138-2146.
- 7 C. Xu, Y. Pan, G. Wan, H. Liu, L. Wang, H. Zhou, S. H. Yu and H. L. Jiang, *J. Am. Chem. Soc.*, 2019, **141**, 19110-19117.